Journal of Photochemistry and Photobiology A: Chemistry 208 (2009) 42–49

Contents lists available at ScienceDirect

Journal of Photochemistry and Photobiology A: Chemistry

journal homepage: www.elsevier.com/locate/jphotochem

Excited state intramolecular proton transfer (ESIPT) from phenol OH (OD) to adjacent "aromatic" carbons in simple biphenyls

Niloufar Behin Aein, Peter Wan*

Department of Chemistry, Box 3065, University of Victoria, Victoria, BC V8W 3V6, Canada

ARTICLE INFO

Article history:
Received 22 May 2009
Received in revised form 8 August 2009
Accepted 14 August 2009
Available online 25 August 2009

Keywords:
Excited state intramolecular proton transfer (ESIPT)
Photosolvolysis
Biphenyl quinone methide

ABSTRACT

This work reports results of further studies on a new class of excited state intramolecular proton transfer (ESIPT), from phenol OH to adjacent aromatic carbon atoms of suitably designed biphenyl systems. For this purpose, a number of 2-phenylphenols **3**–**6** with methyl and methoxy substituents on the adjacent proton accepting phenyl ring were synthesized. In particular, we were also interested in studying the effect of an acetyl (ketone) substituent on the proton accepting ring (biphenyl **7**) and the effect on the photochemistry when the ketone is reduced to alcohol (biphenyl **8**). All compounds except for **7** were found to undergo deuterium exchange (Φ_{ex} = 0.019–0.079) primarily at the 2′-position on photolysis in 1:3 D_2O–CH_3CN. This is consistent with a reaction mechanism involving initial ESIPT from the phenol OH to the 2′-position of the adjacent phenyl ring, to generate a biphenyl quinone methide intermediate which rapidly tautomerizes back to starting material. Biphenyl **8** also undergoes a competing photosolvolysis reaction (overall loss of water). Both photosolvolysis and ESIPT reactions react via isomeric quinone methide intermediates and are best interpreted as arising from an excited singlet state that possesses a large degree of charge transfer character, from the phenol ring to the attached phenyl ring. The failure of **7** to react may be due to two possible reasons: (i) high intersystem crossing rate to a non-polarized triplet excited state and/or (ii) a polarized singlet state that is now much more basic at the carbonyl oxygen. The results are consistent with qualitative examination of calculated HOMOs and LUMOs (AM1).

1. Introduction

Excited state intramolecular proton transfer (ESIPT) reactions are considered to be of fundamental importance and have been studied intensively [1]. In general, ESIPT occurs between heteroatoms such as oxygen and nitrogen that are part of an aromatic or polycyclic aromatic system, to generate a high energy ground state tautomer that readily reverts back to starting material on a very fast time scale. The first extensive studies of ESIPT between a phenol OH and a carbon atom (e.g., the β-carbon of alkene moiety) were first reported by Yates and co-workers for *o*-hydroxystyrene and *o*-hydroxyacetylene [2]. They showed that on photolysis in water, these substrates undergo ESIPT from the phenol to β-carbon atom to give the corresponding tautomer (an *o*-quinone methide), which is then trapped by water to give the corresponding photohydration product.

The first report [3] of an ESIPT between a phenol OH and the carbon atom that is part of an aromatic ring involved 2-phenylphenol (**1**) (Eq. (1)). Photolysis of **1** in D_2O gave extensive deuterium incorporation at the 2′-position (compound **1**-*2′D*) via the proposed quinone methide **2** (or **2**-*2′D*) which is formed via proton transfer from the phenol OH to the 2′-carbon position of the adjacent phenyl ring. The quantum yield for deuterium incorporation for **1** (i.e., formation of **1**-*2′D*) was 0.041 in 1:3 D_2O–CH_3CN. This is a probably a lower limit for the quantum yield of the actual ESIPT step since the intermediate **2**-*2′D* could also lose deuterium (albeit much more slowly than protium) in preference over loss of proton and return to **1**. Thus the actual quantum yield of ESIPT could be somewhat higher indicating that this type of proton transfer is an important non-radiative decay pathway for these types of compounds that has *not* been recognized in the past. This type of ESIPT has now been observed for a variety of related substrates in which the proton accepting ring has been varied to include biphenyl, fluorene, pyridine, naphthalene and anthracene [4].

However, what has been lacking in these studies was information regarding substituent effects on the proton accepting ring in simple 2-phenylphenols and the possibility of competing photosolvolytic chemistry in these simple systems. We have addressed this shortfall by studying relatively simple (and readily synthesized) substituted 2-phenylphenols **3**–**8**. All of these biphenyls have twisted ground state structures (a necessary requirement for the ESIPT discussed in previous work [3]). They were chosen to

* Corresponding author. Tel.: +1 250 721 8976; fax: +1 250 721 7147.
E-mail address: pwan@uvic.ca (P. Wan).

1010-6030/$ – see front matter © 2009 Elsevier B.V. All rights reserved.
doi:10.1016/j.jphotochem.2009.08.004

investigate the effects of steric congestion at the *ortho*-position, possibly resulting in highly twisted ground states (**3** and **4**), the presence of a strong electron donating methoxy group (**4**–**6**), and the effect of a carbonyl substituent which would change the chromophore substantially (**7**). To complete the study, the ketone of **7** was reduced to give the corresponding alcohol to give compound **8**. This removed the ketone moiety and gave a diol that had the potential for a competing photosolvolytic reaction (as shown in related work for these types of compounds [5]), which in fact occurred, in competition with ESIPT (vide infra).

2. Experimental details

2.1. General

^{1}H and ^{13}C NMR spectra were recorded on a Bruker Avance 500 instrument. Mass spectra (MS) were recorded on a Kratos Concept H spectrometer (EI). UV–vis spectra were recorded on a Varian Cary 50 instrument. D_2O and $(CD_3)_2CO$ were purchased from Cambridge Isotope laboratory. Chromatographic separations were carried out by using 200 mL silica gel columns as the stationary phase and hexane/ethyl acetate or dichloromethane/ethyl acetate as mobile phases.

2.2. Materials

The following compounds and reagents were purchased from Aldrich and used as received: 2-bromophenol, 2-methylphenylboronic acid, 4-methylphenylboronic acid, 4-acetylphenylboronic acid, 3,5-dimethylphenylboronic acid, 2,2′-biphenol, $NaBH_4$, $Pd(PPh_3)_4$, CH_3I, polyethylene glycol.

2.2.1. Synthesis

The general procedure for the synthesis of **3** and **5**–**7** employs the well-known Suzuki coupling reaction, adapted from the work of Nam et al. [6], and is described as follows. A mixture of 1 equivalent of 2-bromophenol and 1.2–1.3 equivalents of the phenylboronic acid were dissolved in THF in a 100 mL Schlenk flask. To the reaction mixture were added 2 equivalents of aqueous Na_2CO_3 and the solution purged with N_2 for 20 min. This was followed by addition of 0.03–0.05 equivalents of $Pd(PPh_3)_4$ and refluxed for up to 24 h with monitoring of reaction progress by TLC. After reflux, the solution was cooled to room temperature, dried over anhydrous Na_2SO_4 and filtered through Celite. The pure product was obtained by chromatography on silica using of 10–30% ethyl acetate/n-hexane as eluent.

*2.2.1.1. 2′-Methylbiphenyl-2-ol (**3**).* The yield of this light yellow oil was 1.1 g (71%); ^{1}H NMR ($(CD_3)_2CO$, 500 MHz) δ 7.95 (OH, 1H), 7.17–7.23 (m, 4H), 7.13 (d, 1H, J = 10 Hz), 7.04 (d, 1H, J = 10 Hz), 6.94 (d, 1H, J = 10 Hz), 6.89 (m, 1H), 2.21 (s, CH_3); ^{13}C NMR ($(CD_3)_2CO$, 125 MHz) δ 19.17, 115.46, 119.41, 125.31, 127.07, 127.84, 128.83, 129.17, 129.47, 129.99, 130.66, 136.63, 138.61, 154.10; MS (EI) m/z = 184 for M^+.

*2.2.1.2. 4′-Methoxybiphenyl-2-ol (**5**).* The yield of light yellow oil was 0.78 g (45%). ^{1}H NMR ($(CD_3)_2CO$, 500 MHz) δ 8.17(OH, 1H), 7.53 (dd, 2H, J = 10 and 5 Hz), 7.25 (d, 1H, J = 10 Hz), 7.14 (m, 1H, J = 10 Hz), 6.97(m, 3H), 6.90 (m, 1H), 3.81 (s, CH_3); ^{13}C NMR ($(CD_3)_2CO$, 125 MHz) δ 55.59, 114.37, 116.99, 120.91, 128.92, 129.15, 131.29, 132.07, 155.06, 159.72; MS (EI) m/z = 200 for M^+ (100%).

*2.2.1.3. 3′,5′-Dimethoxybiphenyl-2-ol (**6**).* The yield of light yellow oil was found to be 1.5 g (38%). ^{1}H NMR ($(CD_3)_2CO$, 500 MHz) δ 8.17(OH, 1H), 7.31(dd, 1H, J = 10 and 5 Hz), 7.18 (m, 1H), 6.97(d, 1H, J = 10 Hz), 6.92 (m, 1H), 6.73 (d, 2H, J = 10 Hz), 6.45 (t, 1H, J = 5 Hz), 3.81(s, 6H); ^{13}C NMR ($(CD_3)_2CO$, 125 MHz) δ 55.63, 99.69, 108.34, 117.09, 120.82, 129.39, 129.53, 131.35, 141.55, 155.02, 161.63; MS (EI) m/z = 230 for M^+; HRMS calculated for $C_{14}H_{14}O_3$ 230.0943, found 230.0946.

*2.2.1.4. 4′-Acetylbiphenyl-2-ol (**7**).* The yield of white solid (mp 142–144 °C) was 4.5 g (50%). ^{1}H NMR ($(CD_3)_2CO$, 500 MHz) δ 8.54 (OH, 1H), 8.01 (d, 2H, J = 10 Hz), 7.73 (d, 2H, J = 10 Hz), 7.35 (dd, 1H, J = 10 and 5 Hz,), 7.22 (m, 1H), 7.01 (dd, 1H, J = 10 and 5 Hz), 6.95 (m, 1H), 2.59 (s, CH_3); ^{13}C NMR ($(CD_3)_2CO$, 125 MHz) δ 25.69, 116.17, 120.99, 120.04, 127.19, 127.80, 129.22, 129.29, 130.41, 135.44, 134.52, 154.23, 196.60; MS (EI) m/z = 212 for M^+; HRMS calculated for $C_{14}H_{12}O_2$ 212.0837, found 212.0840.

*2.2.1.5. 2′-Methoxybiphenyl-2-ol (**4**).* This compound was prepared based on a published report [7] but modified by the addition of polyethylene glycol as solvent. In a dry 100 mL one-neck round bottom flask under N_2 was charged with 30 mL of acetone and 10 mL of polyethylene glycol. This was followed by the addition of 2,2′-biphenol (1 equivalent, 8.15 mmol) and methyl iodide (2 equivalents, 16.3 mmol). To this reaction mixture was added K_2CO_3 (0.5 equivalent, 4.07 mmol) and stirred at room temperature for 24 h. The resulting solution was extracted with 3 × 50 mL CH_2Cl_2. Upon evaporation of the organic solvent, the crude material was purified by chromatography on silica (2:1 hexane–CH_2Cl_2), to give **4** as a white solid (mp 42–44 °C) (1.4 g, 85%). ^{1}H NMR ($(CD_3)_2CO$, 500 MHz) δ 7.55 (OH, 1H), 7.33 (m, 1H), 7.23 (dd, 1H, J = 10 and 5 Hz), 7.18 (dd, 1H, J = 10 and 5 Hz), 7.16 (m, 1H), 7.06 (d, 1H, J = 10 Hz), 7.00 (m, 1H), 6.91 (d, 1H, J = 10 Hz), 6.88 (m, 1H), 3.81 (s, CH_3); ^{13}C NMR ($(CD_3)_2CO$, 125 MHz) δ 56.03, 112.27, 117.08, 120.45, 121.57, 127.15, 128.57, 129.40, 129.71, 132.38, 132.63, 155.58, 157.81; MS (EI) m/z = 200 for M^+.

*2.2.1.6. 4′-(1″-Hydroxyethyl)biphenyl-2-ol (**8**).* Alcohol **8** was made via standard $NaBH_4$ reduction of ketone **7** in methanol. The crude white solid was purified by chromatography on silica (5:95 ethyl acetate–CH_2Cl_2) and followed by re-crystallization from ethanol, to give a white solid (mp 114–116 °C). ^{1}H NMR (CD_3CN, 500 MHz) δ 7.50 (d, 2H, J = 10 Hz), 7.40 (d, 2H, J = 10 Hz), 7.26 (dd, 1H, J = 10 and 5 Hz,), 7.20 (m, 1H), 6.97 (dd, 1H, J = 10 and 5 Hz), 6.99 (m, 1H), 6.81 (OH, 1H), 4.84 (m, 1H), 3.20 (d, OH, 1H, J = 5 Hz), 1.41 (d, 3H, J = 10 Hz); ^{13}C NMR (CD_3CN, 125 MHz) δ 26.03, 70.04, 117.03, 121.43, 126.28, 129.43, 129.68, 130.19, 131.64, 138.08, 146.77, 154.69; MS (EI) m/z = 214 for M^+; HRMS Calc. for $C_{14}H_{14}O_2$, 214.0994, found 214.0995.

2.3. Photolysis

2.3.1. General procedure for photochemical exchange of **3**–**6** in D_2O–CH_3CN

All the irradiation experiments were performed in a Rayonet photochemical reactor equipped with 16 lamps (254 nm). The solutions were contained in quartz tubes (100 mL), which were cooled to ≤15 °C with tap water by an internal cold finger. The solutions of 10^{-3} M were prepared and purged with argon 15 min prior to irradiation and continuously during the irradiation. The solutions were prepared by first dissolving the compound in the organic solvent before being mixed with the aqueous component. Photolysis times varied from 5 min to 6 h. Workup involved extraction of the photolysed solution with CH_2Cl_2, followed by drying the combined organic layer over anhydrous Na_2SO_4, and removal of the solvent under reduced pressure. The irradiation products were separated (if necessary) by preparative thin-layer chromatography (TLC) and then analyzed by ^{1}H NMR.

*2.3.2. Photosolvolysis of **8** in H_2O–CH_3OH*

A solution of 20 mg of **8** in 100 mL of 1:1 H_2O:CH_3OH was irradiated for 10 min; the photoproduct was analyzed by ^{1}H NMR, which gave methyl ether **9** (67%); ^{1}H NMR (CD_3CN, 300 MHz) δ 7.50 (d, 2H, J = 6 Hz), 7.40 (d, 2H, J = 6 Hz), 7.26 (dd, 1H, J = 6 and 3 Hz), 7.20 (m, 1H), 6.97 (dd, 1H, J = 6 and 3 Hz), 6.99 (m, 1H), 6.81 (OH, 1H), 4.36 (m, 1H), 3.20 (OCH_3, 3H), 1.41 (d, 3H, J = 9 Hz).

*2.3.3. Photolysis of **8** in D_2O–CH_3OH*

A solution of 20 mg of **8** in 100 mL of 1:1 D_2O:CH_3OH was irradiated for 10 min; the photoproduct was analyzed by ^{1}H NMR, which gave a mixture of monodeuterated **8**-*2′D*, and monodeuterated methyl ether **9**-*2′D*. The mixture was separated by preparative TLC on silica (1:9 ethyl acetate–CH_2Cl_2), to give **8**-*2′D* (25% monodeuterated) and monodeuterated methyl ether 9-2′*D* (60% ether yield, 30% monodeuterated).

2.4. Quantum yields

Quantum yields for deuterium exchange (Φ_{ex}) for **3**–**6**, and **8** were measured using the deuterium exchange reaction of 2,2′-biphenol as a reference [3]. A known amount of compound was dissolved in 1:3 (v/v) D_2O–CH_3CN in a quartz tube and conversions were kept below 30%. This was followed by preparing an equimolar amount of the compound with the known quantum yield and irradiated under the same conditions. Integration from ^{1}H NMR was used to determine the relative conversions of deuterium exchange products.

2.5. General procedure for steady-state and time-resolved fluorescence measurements

The samples were dissolved in CH_3CN and the concentrations adjusted to have optical densities at the excitation wavelengths (273–285 nm) of $\leq$0.1. The measurements were performed at 20 °C on a Photon Technology International (PTI) A-1010 Quanta-Master luminescence spectrometer. Fluorescence quantum yields were determined by comparison of the integral of emission bands with that of Fluorene in CH_3CN (Φ_s = 0.68) [8] was used as the standard for measurement of the fluorescence quantum yields. For fluorescence lifetimes using single photon counting, fluorescence decay histograms were obtained on an Edinburgh OB920 instrument equipped with a hydrogen flash lamp, using the time-correlated single photon counting technique. Histograms of the instrument response functions (using a LUDOX scatterer) and sample decays were recorded until they typically reached 4×10^3 counts in the peak channel.

3. Results and discussion

3.1. Photochemical deuterium exchange

As noted in the initial study of ESIPT from phenol to adjacent aromatic carbon atoms [3], a necessary requirement for observation of this kind of proton transfer is that the phenyl rings of the biphenyl system be twisted such that the phenol OH can interact with the π system of the adjacent phenyl ring. Presumably, this initial hydrogen bonding aligns the phenol OH in the correct trajectory for the eventual migration, along with twisting of the rings to a more planar geometry, and charge transfer from the phenol ring to the adjacent ring [3]. The calculated ground state dihedral angle of the parent **1** is 54° [3]. It would be instructive to calculate dihedral angles for **3**–**8** since two of these compounds have large *o*-substituents that may give rise to much larger dihedral angles. Shown in Fig. 1 is the AM1 optimized ground state geometry for **3**, which turned out to be the most twisted of these compounds,

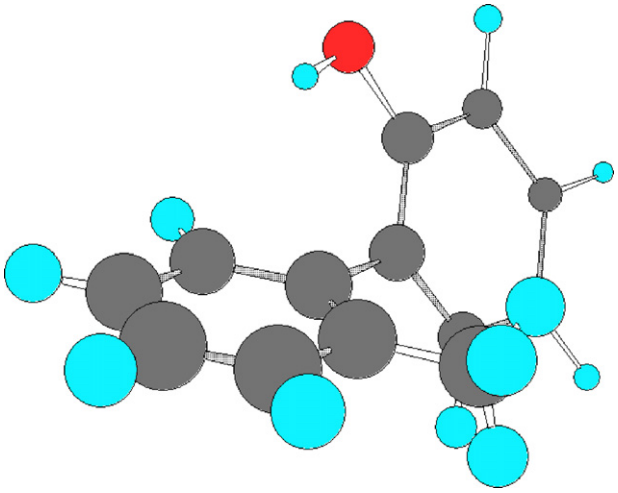

Fig. 1. Optimized geometry of **3** (Chem 3D, AM1/MOPAC) in the ground state, with a dihedral angle of 60° between the phenyl rings.

with a dihedral angle of 60°. Geometry optimization of all of **4**–**8** gave twisted structures with dihedral angles in the 50–53° similar to that calculated for the parent **1** [3]. This may seem surprising for **4** since it has a large OCH_3 substituent at the *ortho*-position. However, on closer inspection, the bulky methyl group is held further away from the adjacent phenyl ring due to the C—O ether bond. The conclusion to be drawn from the above analysis is that the ground state structures of all of **3**–**8** satisfy the geometry required for ESIPT from phenol to the adjacent phenyl ring.

If the proposed ESIPT is the only photochemical pathway for **3**–**8**, then photolysis in H_2O–CH_3CN (or in any other suitable non-deuterated solvent) would not lead to any observable changes in the ^{1}H NMR. Photolysis of all of these compounds in 1:1 H_2O–CH_3CN (10^{-3} M, 254 nm, 16 lamps, 5–60 min) resulted in complete recovery of substrate. Actual ESIPT would only be discernable on photolysis in D_2O–CH_3CN. All of **3**–**6** (and **8**, vide infra) were found to undergo facile deuterium exchange at the 2′-position of the attached phenyl ring (labeled as proton H_a in all of these compounds) followed by a much less efficient exchange at the 4′-position where available (H_c for **3** and **4**; H_b for **6**). Moreover, the efficiency of exchange at the 2′-position in D_2O was independent of D_2O content once all of the phenol OH was converted to OD. For illustration, the details as studied by ^{1}H NMR are presented below for compounds **4** and **6**.

To illustrate the effect of D_2O content on the deuterium exchange efficiency at the 2′-position, photolysis of **4** was carried out at different concentrations of D_2O (in CH_3CN) at a fixed photolysis time (Figs. 2 and 3) (Eq. (2)). Deuterium exchange at the 2′-position was readily observed by ^{1}H NMR (500 MHz). On photolysis, the signal assigned to proton H_a (δ 7.23, dd) decreased in intensity (with no change in splitting pattern), by 20% and 37% in 0.005 M and 0.25 M D_2O, respectively. That deuterium incorporation has taken place at this position was confirmed by the growth of a broad doublet at H_b (δ 6.99) on top of the original dd splitting pattern (but with no net increase in integration), due to the unresolvable coupling with a deuterium (s = 1) now present at the 2′-position. Unresolvable coupling to deuterium was also observed for the proton at H_c (δ 7.34). As more deuterium is incorporated into the 2′-position, the splitting pattern for this proton resembles more of a "triplet" (two superimposed doublets). Due to the low conversion of these experiments, exchange at H_c was not observable (vide infra). No significant changes in coupling were observed for H_d consistent with the distal nature of this proton to the exchange site. Essentially identical observations were made for **3** on photolysis

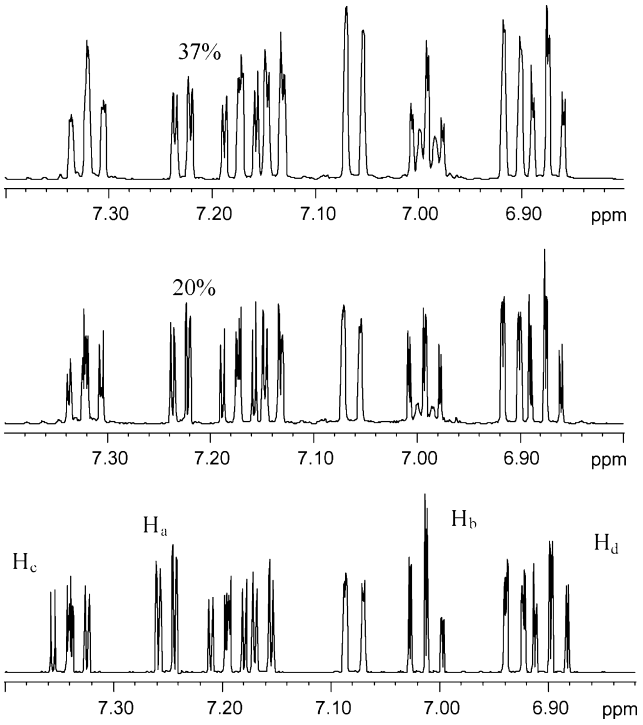

Fig. 2. ^{1}H NMR (500 MHz, $(CD_3)_2CO$) showing the expanded aromatic region of **4** before (bottom) and after photolysis for 5 min (middle, 0.005 M D_2O in CH_3CN; top, 0.25 M D_2O in CH_3CN). ^{1}H NMR integration indicates 20% and 37% deuteration at the 2′-position (H_a) position with no observable exchange at other positions at these conversions.

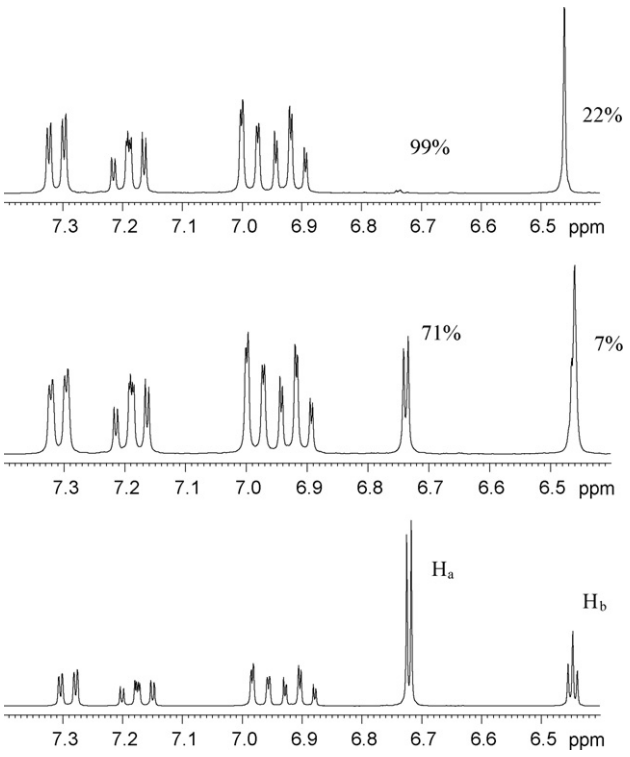

Fig. 4. ^{1}H NMR (300 MHz, $(CD_3)_2CO$) showing the expanded aromatic region of **6** before (bottom) and after photolysis (30 min, middle; 2 h, top) in 1:3 D_2O–CH_3CN. NMR integration shows 71 and 99% deuteration (H_a), and 7 and 22% deuteration (H_b), respectively.

in varying D_2O content since this compound has the same number and pattern of protons on the adjacent phenyl ring (viz., H_a, H_b, H_c and H_d). The ^{1}H NMR analysis of **5** was easier since there are only two protons *ortho* to each other (H_a and H_b). Thus, exchange of H_a in **5** with increasing D_2O content resulted in decrease of this signal and the appearance of a broad singlet at H_b due to unresolved coupling to the deuterium now replacing H_a.

As shown in Fig. 3 for **4**, there is a pronounced increase in deuterium exchange efficiency between 0 and 0.05 M D_2O (in CH_3CN), reaching a plateau region where there is no further increase. The sharp rise in efficiency observed between 0 and 0.05 M D_2O is interpreted as being due to conversion of **4**-*OH* to **4**-*OD*, and that when all of **4**-*OH* has been fully converted to **4**-*OD*, there is no dependence on D_2O content for exchange yield. This is consistent with an exchange mechanism arising via *direct* (unassisted) proton (deuteron) transfer from the phenol OH (OD) to the 2′-carbon of the adjacent phenyl ring in the excited state. The need for an apparent large excess of D_2O (compared to substrate concentration) to reach the plateau region may be associated with a solvent effect; that is, the incorporation of water into CH_3CN at these concentrations may facilitate the proton transfer itself although such details are beyond the scope of this work.

To illustrate the relative efficiency of exchange of the 2′-positions vs 4′-positions in **3**, **4** and **6** (there is no such position in **5**), the results of the photolysis of **6** in 1:3 D_2O–CH_3CN are shown (Figs. 4 and 5). Photolysis quickly led to disappearance of the signal at δ 6.73 (d) due to H_a. Indeed, after 2 h photolysis, this proton had completely exchanged. A much slower exchange was observed for

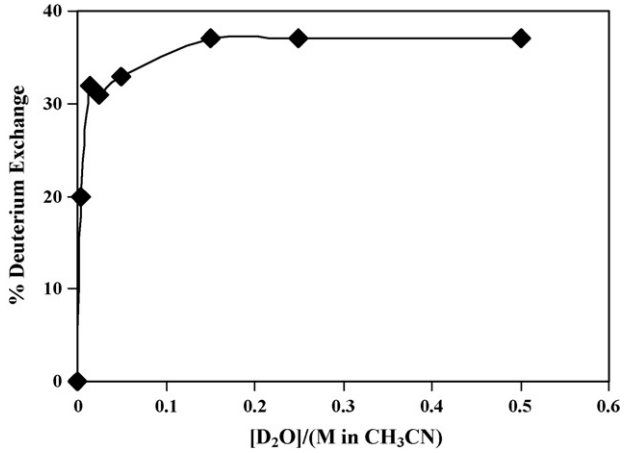

Fig. 3. Plot of %deuterium exchange at the 2′-position of **4** as a function of D_2O content in CH_3CN as measured by ^{1}H NMR (photolysis time 5 min).

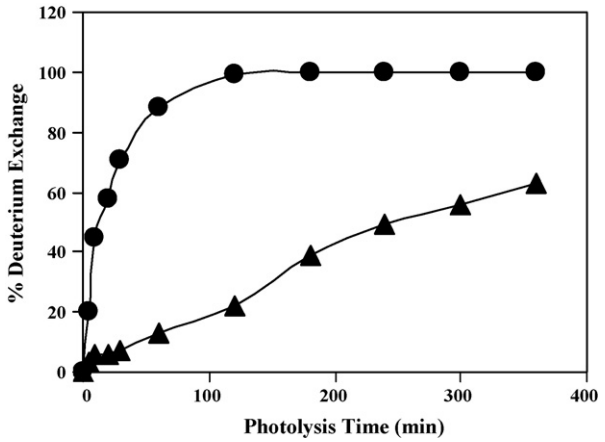

Fig. 5. Plot of %deuterium exchange at the 2′ (●) and 4′ (▲)-positions of **6** vs photolysis time in 1:3 D_2O–CH_3CN, as measured by ^{1}H NMR.

H_b at δ 6.47 (t), being about an order of magnitude less reactive when normalized for the fact that there are two H_a protons for every one of H_b (Fig. 4). The signal at H_b broadens with deuterium incorporation at H_a since coupling to deuterium is not resolvable. In addition, since deuterium incorporation at H_b is much less efficient than at H_a, one can assume that when deuterium is incorporated at H_b, a significant fraction of these molecules will also be deuterated at H_a (Eq. (3)). Note also that the protons on the phenol ring are not affected consistent with deuterium incorporation on the ring not containing the phenol OH. Essentially identical observations were made for **3** and **4**.

Photolysis of **7** in D_2O–CH_3CN for up to 2 h resulted in complete recovery of starting material with no evidence for deuterium incorporation into the benzene ring positions. This is the only compound

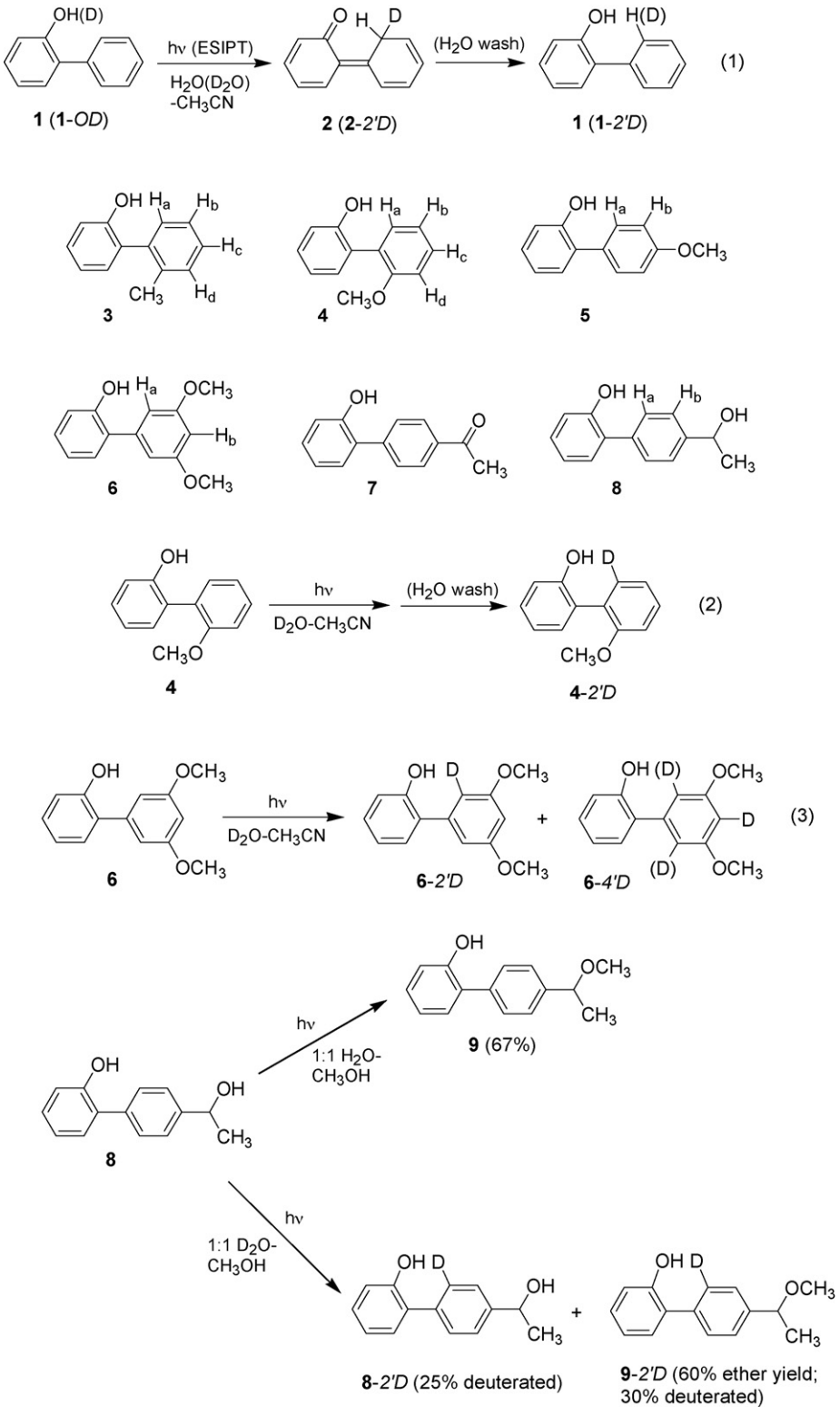

Scheme 1.

Table 1
Photochemical and photophysical parameters for **3**–**6** and **8**.

Compound	λ_{max} (nm)[a]	λ^{fl}_{max} (nm)[b]	Φ_f[c]	Φ_{ex}[d]	τ (ns)[e]
3	273	316	0.47 ± 0.05	0.019 ± 0.002	1.5 ± 0.2
4	280	342	0.39 ± 0.05	0.057 ± 0.004	1.7 ± 0.2
5	283	334	0.47 ± 0.05	0.064 ± 0.004	1.9 ± 0.2
6	285	345	0.14 ± 0.02	0.079 ± 0.002	0.8 ± 0.2
8	285	328	0.39 ± 0.05	0.029 ± 0.004	1.8 ± 0.2

[a] λ_{max} of the longest wavelength absorption band.
[b] λ_{max} of the fluorescence emission band.
[c] Fluorescence quantum yields in neat CH_3CN, measured relative to the reported fluorescence quantum yield for fluorene in CH_3CN (Φ_f = 0.68) [8].
[d] Quantum yields of formation of **3**-*2′D*, **4**-*2′D*, **5**-*2′D*, **6**-*2′D*, and **8**-*2′D* in 1:3 D_2O–CH_3CN. Estimated error is ±10% of the final value. Measured using the quantum yield for deuterium incorporation reported for 2,2′-biphenol [3].
[e] Fluorescence lifetime in neat CH_3CN measured by single photon counting in neat CH_3CN.

with an electron withdrawing group on the phenyl ring adjacent to the phenol. However, it is also an aromatic ketone which is expected to alter the photophysical characteristics of the biphenyl substantially. The failure of this compound to undergo ESIPT to the adjacent phenyl carbons was therefore not surprising and two possible explanations are provided (vide infra).

3.2. Photosolvolysis vs photochemical deuterium exchange of 8

Biphenylphenols of the structural type **8** where there is both a benzyl alcohol and a phenol chromophore on the same molecule have the potential to undergo efficient photosolvolysis via biphenyl quinone methide intermediates [5]. Notwithstanding the photosolvolysis reaction, compound **8** could also undergo ESIPT based on results obtained so far for these types of phenols. Initially, the potential photosolvolysis of **8** was studied in 1:1 H_2O–CH_3OH (10^{-3} M, 254 nm, 10 min) which afforded the methyl ether product **9** in 67% yield (Scheme 1). Does ESIPT compete favourably with this anticipated photosolvolytic process? This question was addressed by photolysis of **8** in 1:1 D_2O–CH_3OH (10^{-3} M, 254 nm, 10 min) which gave recovered **8** that was 25% deuterated at the 2′-position (exchange at H_a, not H_b; formation of **8**-*2′D*) and 60% chemical yield of methyl ether **9** that was 30% deuterated at the 2′-position (formation of **9**-*2′D*) (Scheme 1). The significant extent of deuteration observed in both **8** and **9** even when the exchangeable deuterium content was limited due to the use of CH_3OH (and not CH_3OD) in this experiment shows that ESIPT from the phenol OH to the 2′-position is a major photochemical pathway and competes very well with the photosolvolytic pathway in the solvent system studied.

Finally, quantum yields for deuterium exchange for **3**–**6** and **8** at the 2′-position in 1:3 D_2O–CH_3CN were measured using a secondary reference (2,2-biphenol, Φ_{ex} = 0.034 [3]) and are given in Table 1. Although a detailed kinetic treatment is required in order to assess intrinsic reactivity, a few qualitative observations are in order. All of the phenylphenols with methoxy substituents have the highest quantum yields for deuterium exchange, with compound **6** (two methoxy groups) having the highest yield at 0.079. Thus the presence of an electron donating methoxy group at the proton accepting phenyl ring enhances quantum efficiency. Diol **8** has the lowest quantum yield which is consistent with the operation of a competing photosolvolysis reaction at the benzylic position.

3.3. Fluorescence measurements

Fluorescence parameters for **3**–**6** and **8** are shown in Table 1. Ketone **7** was non-fluorescent consistent with a very fast intersystem crossing to the triplet state for this compound. In general, these biphenyls have high fluorescence efficiencies in organic solvents,

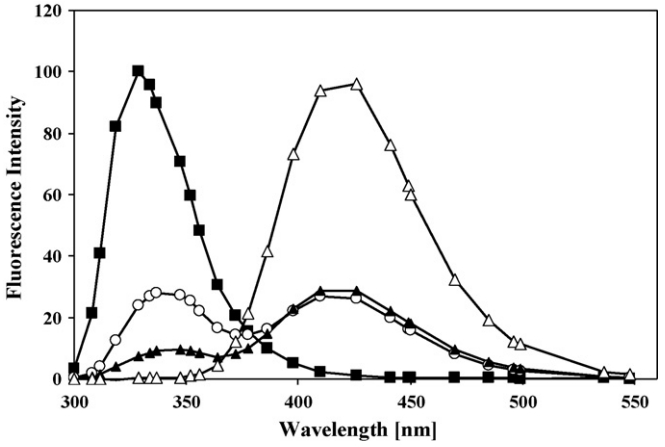

Fig. 6. Fluorescence emission spectra of **8** in various solvents, (■) CH_3CN, (◯) 70:30 (v/v) H_2O–CH_3CN, (▲) 90:10 H_2O:CH_3CN, and (△) pH 12 (100% H_2O). The emission at 420 nm is assigned to the phenolate.

with Φ_f of up 0.47. A comparison of the quantum yields of fluorescence vs deuterium exchange ($\Phi_{ex} \sim 0.02$–0.08) indicates that the ESIPT process is a minor but not insignificant channel, especially given the fact that the quantum yield for actual proton transfer to the 2′-position is greater (by perhaps a factor of 2) than the actual exchange quantum yield. Nevertheless, a casual examination of trends in fluorescence quantum yields would not have revealed the possibility of this additional photochemical pathway without some prior knowledge.

Fluorescence emission of the phenol was quenched on the addition of water with concurrent formation of an easily observable phenolate emission at longer wavelength as shown in Fig. 6 for **8**. The only exception was for **5** which gave very weak phenolate emission on quenching of the phenol emission although it behaved in all respects like the other compounds with respect to deuterium incorporation via ESIPT. High concentrations of water (>5 M) are required for observable fluorescence quenching and formation of the phenolate. Since ESIPT to the 2′-position is independent of water content above 0.1 M H_2O (D_2O), the excited state dissociation of the phenol to phenolate (excited state proton transfer (ESPT) to solvent water) is a photophysical process that is in competition with ESIPT. That is, the phenolate ion that is formed in the ESPT process is probably not involved in the deuterium exchange at the 2′-position.

3.4. Mechanisms of reaction

This work has shown that ESIPT from phenol OH to the 2′-position of an *ortho*-substituted phenyl ring is a reasonably general reaction, with moderate quantum yields. For those compounds with available 4′-positions, a water-mediated ESIPT to this position was also observed but with much less efficiency. As shown in Figs. 7 and 8 for compounds **3** and **6**, respectively, the calculated HOMOs and LUMOs (AM1, Chem 3D/MPOAC) shown substantial migration of electron density (from the phenol ring, with participation of the OH, to the adjacent ring) on promotion of an electron from the HOMO to the LUMO for these compounds. In particular, the substituents (methyl or methoxy) on the proton accepting ring play little or no role in these two MOs. Moreover, it is clear that closer examination shows that the greatest change in electron density occurs for one of the 2′-positions and one of 3′-positions of the proton accepting ring, with these carbons becoming the most basic on excitation.

For a mechanism that involves a direct transfer of the phenol OH proton, transfer to the 2′-position would be highly favoured

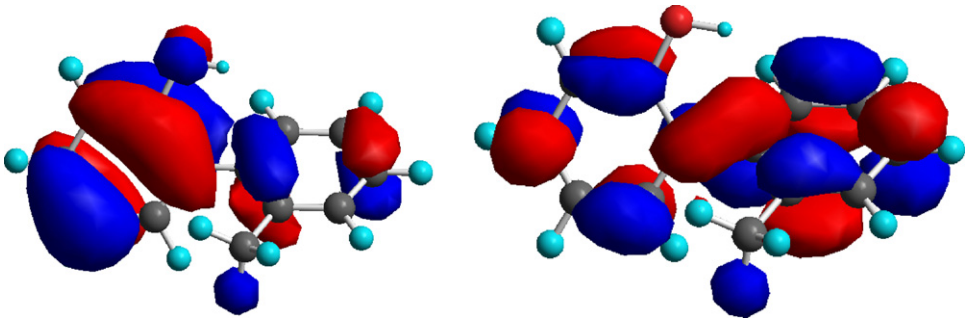

Fig. 7. Calculated (AM1, Chem 3D/MOPAC) HOMO (left) and LUMO (right) for **3**.

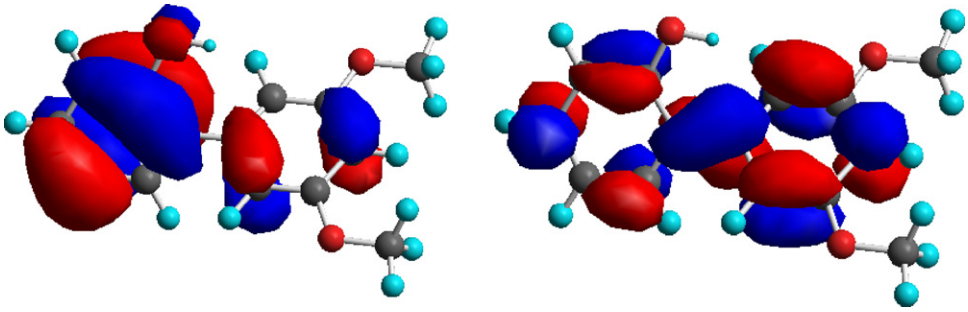

Fig. 8. Calculated (AM1, Chem 3D/MOPAC) HOMO (left) and LUMO (right) for **6**.

since the 3′-position would be too far away for overlap with the OH proton. This mechanism is shown in Scheme 2 for compound **4**. Direct ESIPT would generate quinone methide **4a** which would tautomerize back to the phenol with incorporation of deuterium when D_2O is used. On the addition of water, proton transfer to the 4′-position was eventually observed (but not to the 3′-position). Water provides a mediating agent for transfer of the phenol OH to more distal positions and we propose an intermediate phenolate **4b** which would allow for the proton to be transferred to the 4′-position, to generate quinone methide **4c**. However, transfer to the 3′-position has never been observed in our studies. It is not clear at this time why **4b** would not undergo protonation at the 3′-position except the fact that such a protonation step would generate a high energy non-Kekulé quinone methide intermediate. Thus, one possibility is that proton transfer to this position on the excited state surface would not lead to any stable species on the ground state surface and the transfer is "aborted" although more detailed calculations are required to firm up this speculative proposal.

Calculated HOMOs and LUMOs for **7** and **8** are shown in Figs. 9 and 10, respectively. There is substantial migration of electron density on electron excitation of these two molecules. Notably, for ketone **7**, the migration of charge extends to the carbonyl oxygen, making it basic as well, in addition to the carbon atoms of the adjacent phenyl ring. Thus the lack of any deuterium incorporation at the carbon atoms of **7** on photolysis in D_2O may be due to an ESIPT pathway that exclusively transfers the phenol OH proton to the carbonyl oxygen, mediated by water. This explanation of course does not exclude a simpler explanation in which the triplet excited state of this compound has little or no charge transfer character.

Examination of the HOMO and LUMO of **8** shows that migration of charge from the phenol ring extends to the benzylic C–H proton (of the proton accepting ring), in addition to the phenyl ring carbons. There is also substantial migration of charge to the phenyl ring carbon attached the benzylic carbon. For this compound, ESIPT to the 2′-position was observed but with reduced quantum efficiency compared to the simpler compounds. We also note that this compound has a competing photosovolytic reaction. Scheme 3 shows the proposed mechanisms of reaction for diol **8**. The direct ESIPT process occurs with or without water, to generate quinone methide **8a**. At higher water content, we visualize an intermediate

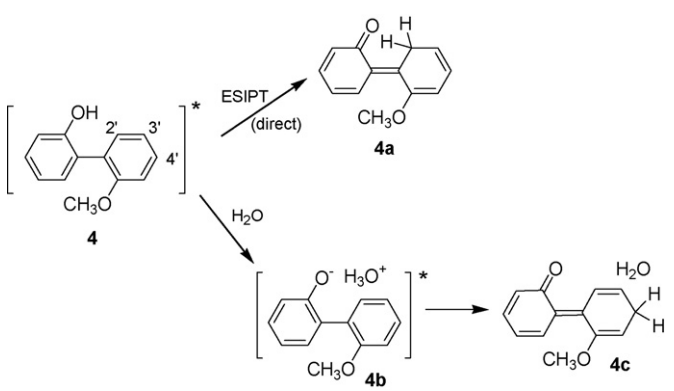

Scheme 2.

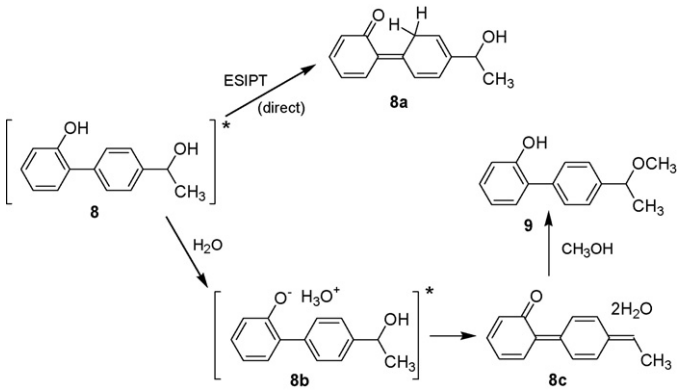

Scheme 3.

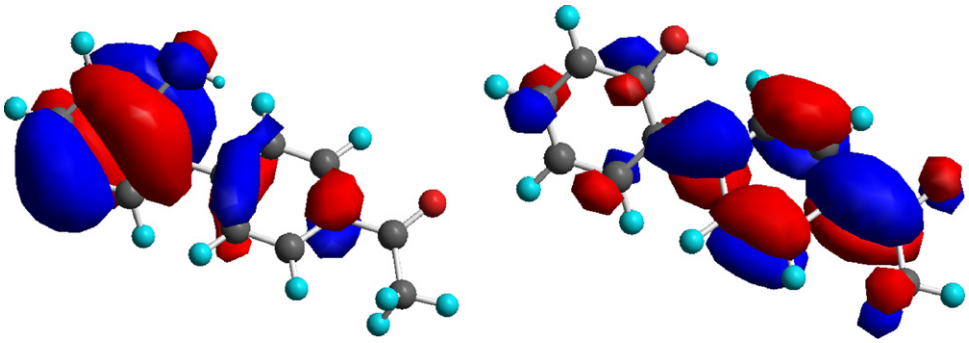

Fig. 9. Calculated (AM1, Chem 3D/MOPAC) HOMO (left) and LUMO (right) for ketone **7**.

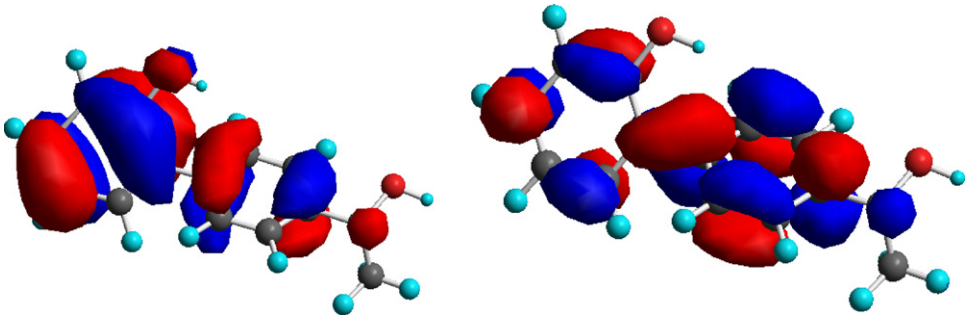

Fig. 10. Calculated (AM1, Chem 3D/MPOAC) HOMO (left) and LUMO (right) for diol **8**.

8b (with one or more water molecules) that allows for the loss of hydroxide ion from the benzylic position with the assistance of the hydronium ion, to generate quinone methide **8c** and hence overall solvolysis (attack at the terminal quinone methide position by CH_3OH) to give **9**. We cannot exclude at this time a mechanism in which the hydronium ion protonates the 4′-position followed by dehydration to form **8c**. However, it would seem reasonable that the enhanced charge at the benzylic C—H and at the carbon atom attached to the benzylic carbon facilitates the expulsion of hydroxide ion (overall dehydration) and hence a photosolvolytic pathway that generates **8c** directly from the phenolate. Note that attack of **8a** by CH_3OH (which might seem reasonable initially) would not lead to any stable product; this quinone methide can only return to starting material **8**. Both ESIPT and photosolvolysis are competitive at high water content although formation of **8a** (ESIPT) would be the exclusive pathway at very low water content or in neat CH_3CN. Herein, we have shown conclusively that charge migration from the phenol to an adjacent phenyl ring can result in two competing photochemical reactions, both involving proton transfer as the primary photochemical step. One can assume that more complex photochemical reactions can be designed based on these findings and these are under study in our laboratory.

Acknowledgments

Support of this research by NSERC (Canada) and the University of Victoria is gratefully acknowledged.

References

[1] (a) S.M. Ormson, R.G. Brown, Prog. React. Kinet. 19 (1994) 45;
(b) D. LeGourrierec, S.M. Ormson, R.G. Brown, Prog. React. Kinet. 19 (1994) 211;
(c) S.J. Formosinho, L.G. Arnaut, J. Photochem. Photobiol. A 75 (1993) 21.
[2] (a) M. Isaks, K. Yates, P. Kalanderopoulos, J. Am. Chem. Soc. 106 (1984) 2728;
(b) P. Kalanderopoulos, K. Yates, J. Am. Chem. Soc. 108 (1986) 6290.
[3] (a) M. Lukeman, P. Wan, J. Chem. Soc. Chem. Commun. (2001) 1004;
(b) M. Lukeman, P. Wan, J. Am. Chem. Soc. 124 (2002) 9458.
[4] (a) M.K. Nayak, P. Wan, Photochem. Photobiol. Sci. 7 (2008) 1544;
(b) M. Flegel, M. Lukeman, P. Wan, Can. J. Chem. 86 (2008) 161;
(c) N. Basarić, P. Wan, Photochem. Photobiol. Sci. 5 (2006) 656;
(d) N. Basarić, P. Wan, J. Org. Chem. 71 (2006) 2677;
(e) M. Flegel, M. Lukeman, L. Huck, P. Wan, J. Am. Chem. Soc. 126 (2004) 7890;
(f) M. Lukeman, P. Wan, J. Am. Chem. Soc. 125 (2003) 1164.
[5] (a) Y. Shi, P. Wan, Can. J. Chem. 83 (2005) 1306;
(b) M. Xu, M. Lukeman, P. Wan, Photochem. Photobiol. 82 (2006) 50–56;
(c) C.-G. Huang, K.A. Beveridge, P. Wan, J. Am. Chem. Soc. 113 (1991) 7676.
[6] H. Nam, B. Boury, S.Y. Park, Chem. Mater. 18 (2006) 5716.
[7] D.C. Harrowven, T. Woodcock, P.D. Howes, Tetrahedron Lett. 43 (2002) 9327.
[8] S.L. Murov, I. Carmichael, G.L. Hug, Handbook of Photochemistry, 2nd ed., Marcel Dekker, New York, 1993.